Two Types of Ca²⁺ Currents with Different Sensitivities to Organic Ca²⁺ Channel Antagonists in Guinea Pig Pancreatic α_2 Cells

PATRIK RORSMAN

From the Department of Medical Cell Biology, Biomedicum, S-751 23 Uppsala, Sweden

ABSTRACT   The possibility that guinea pig pancreatic α_2 cells are equipped with more than one type of Ca²⁺ channel was explored using the patch-electrode voltage-clamp technique. At a holding potential of −100 mV, a slowly developing ($\tau_m \sim$ 5 ms at −40 mV assuming m^2 kinetics) Ca²⁺ current appeared. This conductance first became detectable at potentials of about −60 mV and reached a maximum amplitude of 50–100 pA between −30 and −20 mV. During long depolarizations, it inactivated completely ($\tau_h \sim$ 100 ms at −40 mV). Half-maximal steady state inactivation was observed at about −60 mV. A second, more rapidly developing ($\tau_m \sim$ 2 ms at 0 mV) Ca²⁺ current was observed during pulses to −40 mV and above. It had a peak amplitude of 150–200 pA between 0 and 10 mV, was less dependent on the holding potential, and inactivated very little, even during long pulses. Both conductances were blocked by Co²⁺ but were unaffected by tetrodotoxin. The rapidly developing current differed from the slowly developing one in being sensitive to the antagonists D-600 and nifedipine, conducting Ba²⁺ better than Ca²⁺, increasing upon exposure to forskolin, and showing time-dependent decay (rundown). These findings indicate that the α_2 cells are equipped with two kinds of Ca²⁺ channels.

INTRODUCTION

In the preceding article (Rorsman and Hellman, 1988), a large Na⁺ (500 pA) and a small Ca²⁺ (100 pA) current were described in glucagon-secreting α_2 cells, which account for the depolarizing phase of the action potential. Whereas inhibition of the Na⁺ current only retarded the upstroke velocity of the action potential, the suppression of the smaller Ca²⁺ current had more pronounced effects and action potentials could no longer be elicited. It was suggested that this absolute requirement of extracellular Ca²⁺ for the initiation of the action potential reflects the involvement of a low-threshold Ca²⁺ current (Rorsman and Hellman, 1988). This possibility is pursued in the present investigation and it is

demonstrated that α_2 cells have, in addition to the standard Ca^{2+} current, a second Ca^{2+} current activating at potentials close to the threshold for action potential initiation. This current bears a strong resemblance to a low-voltage–activated Ca^{2+} current previously described in neurons (Carbone and Lux, 1984a, b; Bossu et al., 1985; Nowycky et al., 1985; Fedulova et al., 1985), as well as in other tissues (Armstrong and Matteson, 1985; Bean, 1985; Cota, 1986; De-Riemer and Sakmann, 1986).

METHODS

The methods were as described in the preceding article (Rorsman and Hellman, 1988). The pipettes were filled with intracellular medium F and the bath contained solution D with 10.2 mM Ca^{2+}. Current-voltage (I-V) relationships are shown after compensation for linear leak. Unless otherwise indicated, the pulses applied were 50 ms long and had a frequency of 0.5 Hz.

RESULTS

Evidence for Two Types of Ca^{2+} Channel

Fig. 1 shows the currents that resulted when depolarizing commands were applied from a holding potential of −100 mV. A slowly rising inward current was first observable at −60 mV (not shown). The time courses of the development of the Ca^{2+} current were best fitted by an m^2 form (Hagiwara and Ohmori, 1982) where $m(t) = m_\infty [1 - \exp(-t/\tau_m)]$. The accuracy of the fits is indicated by the circles superimposed on the current traces for −40 and 0 mV. The time constant of activation (τ_m) was found to be 5.3 ± 0.5 ms ($n = 10$) at −40 mV. With increasing voltages, the activation became more rapid, and at 0 mV, the time constant averaged 1.6 ± 0.2 ms ($n = 10$). In the membrane potential range between −40 and −20 mV, there was only a slight increase of the peak amplitude. Beyond −20 mV, the current showed a secondary rise that reached a maximum between 0 and 10 mV (Fig. 1B). The Ca^{2+} currents reversed between 50 and 70 mV, depending on the extracellular Ca^{2+} concentration. These values are much lower than the Ca^{2+} equilibrium potential, which is ~130 mV with the present solutions (extracellular $[Ca^{2+}]$ = 2.6 or 10.2 mM; intracellular $[Ca^{2+}]$ = 0.06 μM). This discrepancy can be explained assuming an extra outward current activating at more positive potentials (Hille, 1984).

As indicated in Fig. 1B, the I-V relationship revealed a "shoulder" at about −40 mV. This shoulder was more prominent in the individual experiments because of a cell-to-cell variation in the membrane potential range at which it was observed (cf. Figs. 2 and 7). Fig. 1, C and D, compares the current responses for holding potentials of −100 or −50 mV. Whereas a pulse to −40 mV elicited a clear current response when held at −100 mV, very little current was observed upon depolarization to the same potential from −50 mV (Fig. 1C). The situation was different during pulses up to 0 mV. In this case, the current evoked from −50 mV was almost as big as that obtained at a holding potential of −100 mV. The simplest interpretation of this is that, at a holding potential of −50 mV, a low-threshold component of Ca^{2+} conductance inactivates, so that only the "standard" high-threshold current remains to be activated. This idea is supported

by the *I-V* relationship obtained when pulsing from −50 mV (Fig. 1*B*). In this case, no shoulder was detectable at low potentials, and the maximum amplitude was reached at 10 mV, coincident with the peak of the secondary rise found when holding at −100 mV.

Separation of Low- and High-Threshold Ca^{2+} Conductances

Fig. 2 shows an attempt to separate the *I-V* relationships of the two Ca^{2+} conductances. In adopting the method of Bean (1985), the current responses
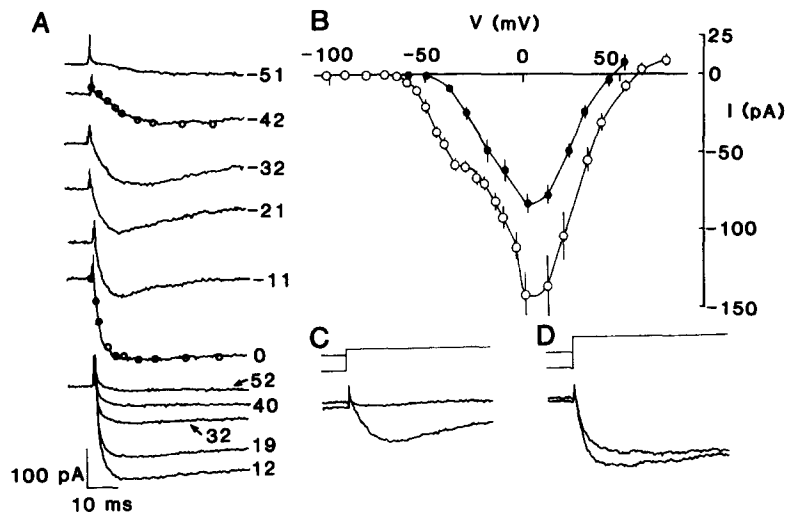

FIGURE 1.   Two types of Ca^{2+} currents in α₂ cells. (*A*) The cell was clamped at −100 mV. Depolarizing voltage pulses were going to the potentials indicated to the right of the traces. Note the small increase in peak current size in the membrane potential range −40 to −20 mV. The circles superimposed on current traces for −40 and 0 mV show the predicted time courses of current activation assuming m^2 kinetics. The values of τ_m for the currents shown are 5.9 and 2.1 ms. (*B*) *I-V* relationship of peak inward Ca^{2+} current using a holding potential of −100 (○) or −50 (●) mV. Note the shoulder at about −35 mV observed with a holding potential at −100 mV. Mean values ± SEM of seven experiments. (*C*) Pulses going to −40 mV from a holding potential of −100 or −50 mV. No current response is elicited when holding at −50 mV. (*D*) Pulses going to 0 from a holding potential of −100 or −50 mV. The current response is almost as big when going from −50 mV as when pulsing from −100 mV.

from a holding potential of −50 mV (open circles) were subtracted from those obtained when holding at −100 mV (filled circles). The procedure is illustrated in Fig. 2, *A* and *B*, for two sets of current responses obtained at different membrane potentials in a cell with an unusually large proportion of the low-threshold component. The current remaining after subtraction (filled triangles) represents the current that can be activated from −100 but not from −50 mV. After the respective amplitudes are plotted against the voltage (Fig. 2*C*), it can be seen that the low-threshold current is characterized by a broad peak at about

−20 mV (it varies between −30 and −20 mV in different cells) and then a slow decline with increasing voltages. In some cells, a secondary rise of the current could still be observed after subtraction for potentials exceeding zero. It is possible that this reflects the existence in the α_2 cell membrane of a third type of Ca^{2+} current. In requiring both a negative holding potential and large depolarizing commands, this current resembles the N-current recently observed in neurons (Nowycky et al., 1985).

Inactivation of Ca^{2+} Currents

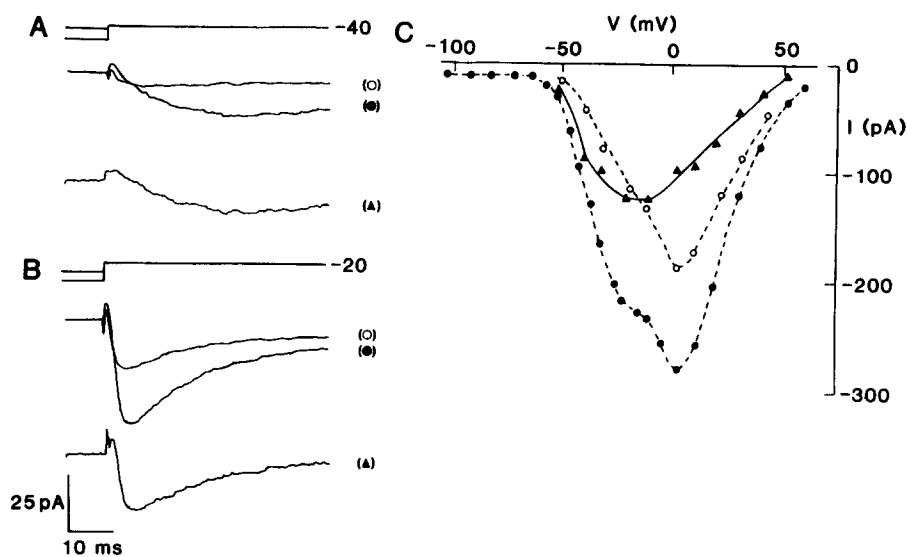The low-threshold Ca^{2+} current differed from the standard type not only with

FIGURE 2.   Separation of low- and high-threshold Ca^{2+} currents. (A and B) Depolarizing pulses were applied from a holding potential of either −100 (●) or −50 (○) mV. The current responses were subtracted from each other and the residual current (▲) was assumed to represent the low-threshold Ca^{2+} conductance. The procedure is illustrated for pulses going to −40 and −20 mV. (C) I-V relationships are shown for the total (●), high-threshold (○), and low-threshold (▲) Ca^{2+} currents.

respect to its voltage dependence but also in showing clear inactivation. Fig. 3A illustrates this difference. Pulses to −42 and 0 mV were applied to activate either the low-threshold conductance or both the low- and high-threshold conductances, respectively. Whereas the pulse going to −42 mV produced a current inactivating completely within 200 ms, the current response to a pulse going to 0 mV did not inactivate more than could be accounted for by the low-threshold component. Since the standard Ca^{2+} conductance needed several seconds to inactivate completely, it was seen as a sustained inward current during long pulses (cf. Fig. 6A). The time courses of the inactivation of the low-threshold Ca^{2+} current could be fitted to a single exponential (Eq. 1 in Rorsman and Hellman, 1988), neglecting some initial deviation. The time constant of inactivation (τ_h) decreased with more

positive voltages, being 209 ± 21 ms ($n = 8$) at -50 mV and 97 ± 10 ms ($n = 8$) at -40 mV. It is unlikely that the inactivation observed reflects the activation of a remaining, slowly developing, outward K$^+$ current. First, the delayed rectifying K$^+$ current in α_2 cells displays appreciable activation only at potentials beyond -20 mV (Fig. 4 in Rorsman and Hellman, 1988), whereas the inactivation of the Ca^{2+} current had already occurred at -50 mV. Second, after the holding potential was shifted to -50 mV, no inactivating component was observable even during large depolarizing pulses, which would be expected if it resulted from the development of an outward current.
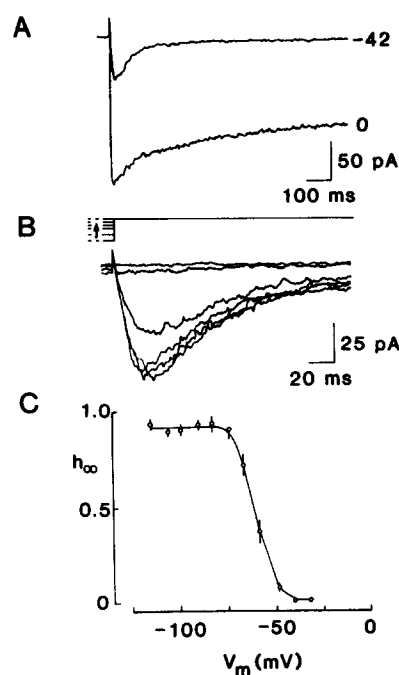

FIGURE 3. Inactivation of Ca^{2+} currents. (A) Inward currents during long (1 s) depolarizing pulses going to -42 and 0 mV. The pulse to -42 mV elicited a current, which inactivated completely. Pulsing to 0 revealed a non-inactivating component (cf. panels A and B in Fig. 6). The pulse frequency was 0.33 Hz. (B) The cell was subjected to 2-s-long voltage pulses between -123 and -25 mV before applying a 200-ms standard pulse going to -40 mV. The pulse frequency was 0.20 Hz. Currents observed during the standard pulse after conditioning pulses to (from top to bottom) -40, -50, -60, -70, -90, and -110 mV are shown. (C) Inactivation curve of low-threshold Ca^{2+} current. Current size evoked after a prepulse to -123 mV was taken as unity. The relative peak amplitude (h_∞) is plotted against the respective conditioning membrane potentials (V_m). Mean values $\pm$ SEM for eight separate experiments.

In Fig. 3B, the voltage dependence of the steady state inactivation of the low-threshold current was studied in more detail by applying a two-pulse protocol with long prepulses (2 s) followed by a standard pulse to -40 mV. The currents obtained during the test pulse were clearly inactivating and had completely disappeared within 200 ms. As the conditioning prepotentials became more positive than -80 mV, less current of the low-threshold type could be activated. After a prepulse to -45 mV, no current remained, which indicates complete inactivation during the conditioning prepulse. Fig. 3C shows the normalized inactivation (h_∞) curve. The process of inactivation occurred in a narrow membrane potential range (between -70 and -50 mV). Using the observed experi-

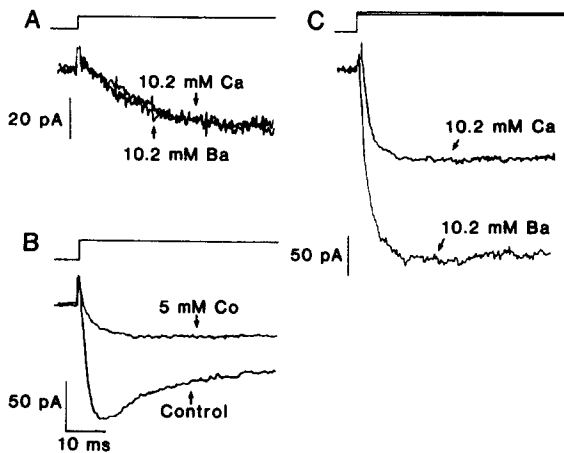FIGURE 4. Effects of Ba²⁺ and Co²⁺ on Ca²⁺ current. Cells were held at −100 mV, and depolarizing commands were applied to activate the low- and high-threshold Ca²⁺ currents, respectively. (A) Depolarizing pulses to −50 mV were used to monitor changes in the low-threshold Ca²⁺ current. Note the lack of effect when Ba²⁺ is used as the charge carrier instead of Ca²⁺. (B) Increase of the high-threshold Ca²⁺ current after substitution of Ca²⁺ with Ba²⁺. Pulses going to 0 for Ca²⁺ and −15 mV for Ba²⁺ to compensate for shift of voltage dependence. (C) Effects of 5 mM Co²⁺ on the Ca²⁺ current in the presence of 10.2 mM Ca²⁺. Pulses going to −10 mV.

mental data in Eq. 2 of the preceding article, values for V_h and k_h of −61 ± 1 and 6 ± 1 mV, respectively (best values ± SEE of eight experiments), were obtained.

Interaction of Ba²⁺ and Co²⁺ with the Ca²⁺ Currents

Whereas equimolar substitution of Ca²⁺ with Ba²⁺ resulted in a doubling of the peak inward current evoked by large voltage steps (Fig. 4B), no such increment was observed when the low-threshold component was selectively activated by pulses going to −50 mV. Substituting Ba²⁺ for Ca²⁺ had little effect, if any, on the time courses of either of the conductances, and the current traces superimposed at the lower potential. These findings suggest that Ba²⁺ and Ca²⁺ are about equally permeant through the low-threshold Ca²⁺ channel, but that Ba²⁺ is conducted better by the high-threshold Ca²⁺ current. Such a difference in the selectivity of the two Ca²⁺ channels has previously been demonstrated in other cell types (Bean, 1985; Fedulova et al., 1985). However, from the present data it is impossible to be completely sure about this point in α_2 cells, since the fraction
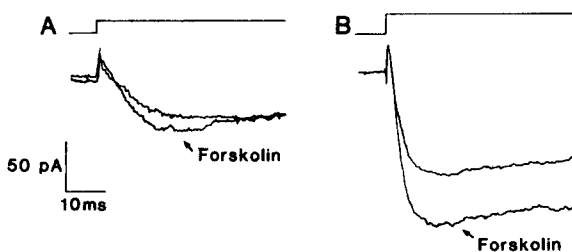

FIGURE 5. Forskolin-induced increase of Ca²⁺ currents in an α_2 cell. The cell was held at −100 mV with depolarizing pulses going to −40 mV to activate the low-threshold Ca²⁺ current (A) and to −10 mV to monitor changes in the high-threshold Ca²⁺ current (B). Currents are shown under control conditions (upper traces) and after 2 min of exposure to 10 μM forskolin (lower traces). The action of forskolin was most pronounced during the large pulse.

of open channels could vary in the two solutions. Tail current analysis or single-channel recordings would be required to exclude this possibility. Ba^{2+} increased the observed current only in the absence of Ca^{2+}. When the Ba^{2+}-containing solution was added to the bath, with resultant mixing of Ba^{2+} and Ca^{2+}, there
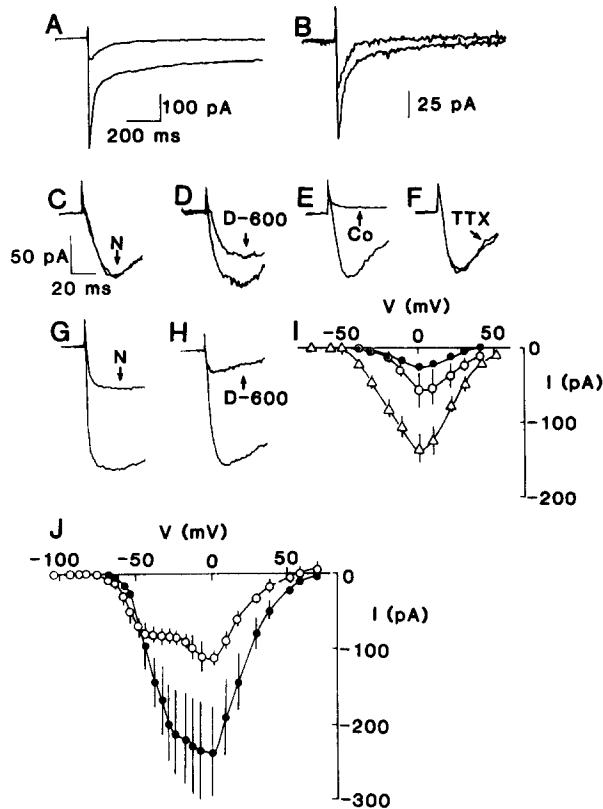
FIGURE 6. Different sensitivities of the two Ca^{2+} currents to D-600 and nifedipine. (*A* and *B*) 1-s pulses to −42 mV (upper traces) and 2 mV (lower traces) were applied in the absence (*A*) or presence (*B*) of 25 μM D-600 from a holding potential of −100 mV. The pulse frequency was 0.33 Hz. Note the existence of inactivating and sustained components in *A*. In the presence of D-600, only the spiky component remained. Different ordinate scales are used in *A* and *B*. In *C–F*, pulses to −40 mV were applied at rates of 0.20–0.33 Hz from a holding potential of −100 mV. (*C*) Lack of effect of 15 μM nifedipine (N). (*D*) Moderate reduction of inward current in the presence of 25 μM D-600. (*E*) Suppression of the inward current after addition of 5 mM Co^{2+}. (*F*) Lack of action of 2.5 μg/ml TTX. In *G* and

H, pulses are going to 0 from a holding potential of −50 mV. The pulse rates were 0.20–0.33 Hz with a duration of 50 ms. (*G*) Current responses before and after addition of 15 μM nifedipine (N). (*H*) Inward currents before and after addition of 25 μM D-600. In *C–H*, the lower traces are the controls. (*I*) *I-V* relationships obtained from a holding potential of −50 mV under control conditions (△) and after the addition of 15 μM nifedipine (○) or 25 μM D-600 (●). Mean values ± SEM for seven (△), four (●), and three (○) experiments. (*J*) *I-V* relationships obtained from a holding potential of −100 mV under control conditions (●) and after adding 15 μM nifedipine (○). Note prominent shoulder on *I-V* relationship between −45 and −20 mV seen in the presence of the antagonist. Mean values ± SEM for three separate experiments. Similar *I-V* relationships were obtained with D-600 (not shown).

was a transient inhibition (50%) of the inward current (cf. Almers and McCleskey, 1984; Hess and Tsien, 1984). Fig. 4*C* shows that 5 mM Co^{2+} suppressed most of the Ca^{2+} current recorded in the presence of 10.2 mM Ca^{2+}. The block was reversible and equally efficient at all voltages (cf. Fig. 6*E*).

Forskolin Potentiation of the Ca^{2+} Current

Forskolin, a stimulator of adenylate cyclase, increased the Ca^{2+} current in some α_2 cells. The action was most pronounced for the high-threshold component (Fig. 5B), and only a moderate increase was observed for the low-threshold current (Fig. 5A). The difficulties in showing an effect of forskolin in all α_2 cells may be attributed to various degrees of washout of the intracellular compartment.

Different Sensitivities of the Two Ca^{2+} Currents to Antagonists

Fig. 6A shows the Ca^{2+} currents activated during pulses to −42 or 2 mV from a holding potential of −100 mV. As already described, the currents produced by the pulse to the lower potential inactivate completely, but the larger step produces currents that can be classified into a transient and a more sustained component. Whereas the low-threshold component was still present after addition of 25 μM
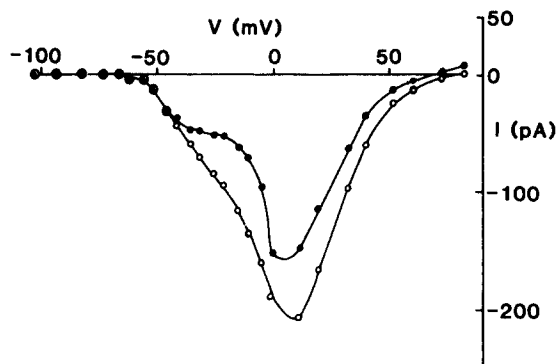

FIGURE 7. Effects of rundown on Ca^{2+} current. I-V relationships of the Ca^{2+} current in an α_2 cell 2 (○) and 10 (●) min after establishing the whole-cell mode. Note the shoulder between −40 and −20 mV, which becomes more prominent with time. Whereas the current size remained unaltered up to about −40 mV, it was reduced at more positive potentials.

D-600, the sustained part was almost completely blocked (Fig. 6B). In Fig. 6, C–F, depolarizing pulses to −40 mV were applied from a holding potential of −100 mV. As can be seen, 15 μM nifedipine did not affect the resultant Ca^{2+} current and 25 μM D-600 reduced its size by as little as 40%. While Co^{2+} abolished the current, the Na^+ channel blocker tetrodotoxin (TTX) had no effect. Although Ca^{2+} antagonists did not affect the low-threshold component, they effectively suppressed the high-threshold Ca^{2+} currents obtained when pulses to 0 mV were applied from a holding potential of −50 mV (Fig. 6, G and H). As shown in Fig. 6I, the inhibition was equally efficient at all voltages between −50 and 50 mV. This differs from the I-V curves obtained when pulses were applied from a holding potential of −100 mV. In this case, nifedipine was without notable action up to −40 mV. At higher potentials, the block became more pronounced, revealing a prominent shoulder between −40 and −20 mV. Qualitatively similar results were obtained in the presence of D-600 (not shown). These findings demonstrate that the two Ca^{2+} conductances of the α_2 cells are differently affected by antagonists, in accord with results from other tissues (Bean, 1985; Boll and Lux, 1985; Fedulova et al., 1985; Cognard et al., 1986; Bossu and Feltz, 1986).

Sensitivity of the Two Ca^{2+} Currents to Rundown

In many cells, the shoulder of the *I-V* relationship was not detectable just after establishing the whole-cell mode, but appeared later. This is illustrated in Fig. 7, which shows the *I-V* relationships shortly after creating the whole-cell configuration (filled circles) and 8 min later (open circles). The shoulder became more prominent with time and the *I-V* relationship recorded at the later time displays a clear hump at potentials between −40 and −20 mV. Furthermore, the maximal magnitude of the Ca^{2+} current had decreased during the 8 min. An explanation for the appearance of the low-threshold component is that it was initially obscured by the large, high-threshold Ca^{2+} current. After partial rundown of the latter component, the low-threshold component became apparent in a way similar to that seen after suppressing the standard type of Ca^{2+} current with Ca^{2+} antagonists (Fig. 6). The current size at −40 mV, i.e., the potential specific for the low-threshold current, was not changed during the 8 min. In accordance with what has been demonstrated in other cell types (Fedulova et al., 1985; Nilius et al., 1985; Cota, 1986; DeRiemer and Sakmann, 1986), it therefore seems likely that the low-threshold Ca^{2+} current is metabolically more stable and consequently less prone to rundown than the classic Ca^{2+} current.

DISCUSSION

The present investigation describes two types of Ca^{2+} conductance in α_2 cells. The more prominent is characterized by showing little inactivation, being less dependent on the holding potential, conducting Ba^{2+} better than Ca^{2+}, being blocked by Ca^{2+} antagonists such as nifedipine, and being susceptible to rundown. This Ca^{2+} current is probably identical to the standard L-type Ca^{2+} current (terminology by Nowycky et al., 1985) previously identified in numerous tissues, including pancreatic β cells (Satin and Cook, 1985; Rorsman and Trube, 1986). This Ca^{2+} current serves the purpose of rapidly injecting Ca^{2+} into the cell, thus leading to an increased intracellular Ca^{2+} with the resulting initiation of (glucagon) secretion. However, α_2 cells possess also a second type of conductance, which differs from the L-type in requiring a more negative holding potential, conducting Ba^{2+} and Ca^{2+} equally well, inactivating rapidly, and not being affected by dihydropyridines. This Ca^{2+} conductance, termed T-type (Nowycky et al., 1985), activates at more negative membrane potentials than are required for the L-type. The inactivating behavior, as well as the voltage dependence of this Ca^{2+} current, resemble those of the Na$^+$ current recorded from α_2 cells (Rorsman and Hellman, 1988). However, the low-threshold Ca^{2+} conductance described here cannot be explained by Ca^{2+} movements through Na$^+$ channels since it persists in the presence of a concentration of TTX found to abolish the Na$^+$ current. The experiments showing differences in the sensitivity to Ca^{2+} channel antagonists suggest that the two currents arise from different channel types. In fact, the discovery of a Ca^{2+} channel resistant to D-600 in α_2 cells might explain why verapamil in some studies has been reported to have no effect on glucagon secretion (Luyckx and Lefèbvre, 1976).

Catecholamines play an important role in the rapid adjustments of various metabolic pathways to physiological demands during stress. It is well-established

that β-adrenergic stimulation of the α_2 cells stimulates the secretion of glucagon (Luyckx, 1983). Although the processes involved are not fully elucidated, it now seems clear that these actions are mediated by intracellular cyclic AMP (Schuit and Pipeleers, 1986). The situation is reminiscent of that in myocardium, where there is a cyclic AMP–induced increase of the Ca^{2+} current within seconds after exposure to β-adrenergic agonists (Reuter and Scholz, 1977; Reuter, 1983; Tsien, 1983). To see whether a similar mechanism could account for the effect of β-adrenergic stimulation in the α_2 cells, the Ca^{2+} current was recorded before and after an increase in the cytoplasmic cyclic AMP levels. Cytosolic cyclic AMP was increased by exposing the α_2 cell to the adenylate cyclase activator forskolin. This procedure enhanced the high-threshold Ca^{2+} current. Thus, during β-adrenergic stimulation, each action potential will be associated with an increased influx of Ca^{2+} into the α_2 cell, leading to a build-up of intracellular Ca^{2+} and an ensuing acceleration of glucagon release.

Low-threshold Ca^{2+} currents have been observed mostly in tissues with a high basal electrical activity, such as neurons (Carbone and Lux, 1984a, b), heart (Bean, 1985; Nilius et al., 1985) and pituitary cells (DeRiemer and Sakmann, 1986), and skeletal muscle (Cognard et al., 1986), and have been suggested to be involved in the regulation of the electrical activity of excitable cells (Llinàs and Jahnsen, 1982; Armstrong and Matteson, 1985; Fedulova et al., 1985). Recent membrane potential recordings from α_2 cells have demonstrated an unconditional requirement for extracellular Ca^{2+} in the generation of the action potentials (Rorsman and Hellman, 1988). The T-type Ca^{2+} current described here in α_2 cells starts activating at about -60 mV, which is close to the threshold of action potential initiation. It is consequently tempting to ascribe a pacemaking role to the low-threshold Ca^{2+} current in α_2 cells. The α_2 cells have a high input resistance (Rorsman and Hellman, 1988). It is therefore easy to envisage how even small current fluctuations, e.g., those of single openings of channels, can occasionally result in a depolarization large enough to activate the T-type Ca^{2+} current, leading to a more marked depolarization and the initiation of an action potential. This concept would be consistent with the occurrence of spontaneous action potentials under basal conditions and explain why a small depolarization, such as that obtained by applying arginine (Rorsman and Hellman, 1988), has such a pronounced effect on the action potential frequency.

REFERENCES

Almers, W., and E. W. McCleskey. 1984. Non-selective conductance in calcium channels of frog muscle: calcium selectivity in a single-file pore. *Journal of Physiology.* 353:589–609.

Armstrong, C. M., and D. R. Matteson. 1985. Two distinct populations of calcium channels in a clonal line of pituitary cells. *Science.* 227:65–67.

Bean, B. P. 1985. Two kinds of calcium channels in canine atrial cells. Differences in kinetics, selectivity and pharmacology. *Journal of General Physiology.* 86:1–30.

Boll, W., and H. D. Lux. 1985. Action of organic antagonists of neuronal calcium currents. *Neuroscience Letters.* 56:335–339.

Bossu, J. L., and A. Feltz. 1986. Inactivation of the low-threshold transient calcium current in rat sensory neurones: evidence for a dual process. *Journal of Physiology.* 376:341–357.

Bossu, J. L., A. Feltz, and J. M. Thomann. 1985. Depolarization elicits two distinct calcium currents in vertebrate sensory neurons. *Pflügers Archiv.* 403:360–368.

Carbone, E., and H. D. Lux. 1984a. A low voltage-activated, fully inactivating Ca channel in vertebrate sensory neurons. *Nature.* 310:634–650.

Carbone, E., and H. D. Lux. 1984b. A low voltage-activated calcium conductance in embryonic chick neurons. *Biophysical Journal.* 46:413–418.

Cognard, C., M. Lazdunski, and G. Romey. 1986. Different types of Ca^{2+} channels in mammalian skeletal muscle cells in culture. *Proceedings of the National Academy of Sciences.* 83:517–521.

Cota, G. 1986. Calcium channel currents in pars intermedia of the rat pituitary gland. Kinetic properties and washout during dialysis. *Journal of General Physiology.* 88:83–105.

DeRiemer, S. A., and B. Sakmann. 1986. Two calcium currents in normal rat anterior pituitary cells identified by a plaque assay. *Experimental Brain Research.* Series 14. 139–154.

Fedulova, S. A., P. G. Kostyuk, and N. S. Veselovsky. 1985. Two types of calcium channels in somatic membranes of new-born rat dorsal root ganglion neurones. *Journal of Physiology.* 359:431–446.

Hagiwara, S., and H. Ohmori. 1982. Studies on calcium channels in clonal pituitary cells with patch electrode voltage clamp. *Journal of Physiology.* 331:231–252.

Hess, P., and R. W. Tsien. 1984. Mechanisms of ion permeation through Ca^{2+} channels. *Nature.* 309:453–456.

Hille, B. 1984. Ionic Channels of Excitable Membranes. Sinauer Associates, Inc., Sunderland, MA. 76–98.

Llinàs, R., and H. Jahnsen. 1982. Electrophysiology of mammalian thalamic neurones *in vitro.* *Nature.* 297:406–408.

Luyckx, A. S. 1983. Pharmacologic compounds affecting glucagon secretion. *In* Handbook of Experimental Pharmacology. P. J. Lefèbvre, editor. Springer-Verlag, Berlin. 66/II:175–201.

Luyckx, A. S., and P. J. Lefèbvre. 1976. Pharmacological compounds affecting plasma glucagon levels in rats. *Biochemical Pharmacology.* 25:2703–2708.

Nilius, B., P. Hess, J. B. Lansman, and R. W. Tsien. 1985. A novel type of cardiac calcium channel in ventricular cells. *Nature.* 316:443–446.

Nowycky, M. C., A. P. Fox, and R. W. Tsien. 1985. Three types of neuronal calcium channel with different calcium agonist sensitivity. *Nature.* 316:440–443.

Reuter, H. 1983. Calcium channel modulation by neurotransmitters, enzymes and drugs. *Nature.* 301:569–574.

Reuter, H., and H. Scholz. 1977. The regulation of the calcium conductance of cardiac muscle cells by adrenaline. *Journal of Physiology.* 264:49–62.

Rorsman, P., and B. Hellman. 1988. Voltage-activated currents in guinea pig pancreatic α_2 cells. Evidence for Ca^{2+}-dependent action potentials. *Journal of General Physiology.* 91:223–242.

Rorsman, P., and G. Trube. 1986. Calcium and delayed potassium currents in mouse pancreatic
    β-cells under voltage-clamp conditions. *Journal of Physiology.* 374:531–550.

Satin, L. S., and D. L. Cook. 1985. Voltage-gated inward currents in pancreatic islet B-cells.
    Pflügers Archiv. 404:385–387.

Schuit, F. C., and D. G. Pipeleers. 1986. Differences in adrenergic recognition by pancreatic
    A and B cells. *Science.* 232:341–358.

Tsien, R. W. 1983. Calcium channels in excitable cell membranes. *Annual Review of Physiology.*
    45:341–358.